RSC Advances

PAPER

View Article Online
View Journal | View Issue

Cite this: *RSC Adv.*, 2023, **13**, 8153

Hydrolysis of regenerated cellulose from ionic liquids and deep eutectic solvent over sulfonated carbon catalysts†

Han Ung Kim, Jong Wha Kim, Sumin Seo and Jungho Jae *

The efficient hydrolysis of cellulose into its monomer unit such as glucose or valuable cello-oligosaccharides is the critical step for the cost-effective production of biofuels and biochemicals. However, the current cellulose hydrolysis process involves high energy-demanding pretreatment (*e.g.*, ball-milling) and long reaction times (>24 h). Herein, we investigated the feasibility of the dissolution/regeneration (DR) of cellulose in ionic liquids (ILs) and deep eutectic solvent (DES) as an alternative to ball-milling pretreatment for the effective hydrolysis of cellulose. Because chlorine-based solvents were reported to be the most active for cellulose pretreatment, [EMIM]Cl and [DMIM]DMP were selected as the IL molecules, and choline chloride–lactic acid and choline chloride–imidazole were selected as the DES molecules. The level of the crystallinity reduction of the regenerated cellulose were analyzed using XRD and SEM measurements. The hydrolysis kinetics of the regenerated cellulose from ILs and DES were examined at 150 °C using sulfonated carbon catalysts and compared with those of the ball-milled cellulose. Overall, the cellulose pretreatment using the ILs and the DES had superior kinetics for cellulose hydrolysis to the conventional ball milling treatment, suggesting a possibility to replace the current high energy-demanding ball-milling process with the energy-saving DR process. In addition, the utilization of supercritical carbon dioxide-induced carbonic acid as an *in situ* acid catalyst for the enhanced hydrolysis of cellulose was presented for the first time.

Received 25th December 2022
Accepted 23rd February 2023

DOI: 10.1039/d2ra08224a

rsc.li/rsc-advances

Introduction

Due to their abundance and carbon neutrality, lignocellulosic biofuels and biochemicals are receiving much attention as a practical solution for realizing the carbon neutral economy.[1–4] Various thermochemical processes such as pyrolysis and catalytic upgrading have been developed for the valorization of biomass or cellulose-derived compounds to drop-in biofuels and petrochemical feedstocks.[5–9] However, recent technoeconomic analysis results showed that the majority of these processes lack cost competitiveness compared to fossil fuels.[10,11] The major reason for the high price of the lignocellulosic biofuels is due to very slow and inefficient depolymerization processes of cellulose to processable monomer units such as glucose.[12] For instance, the hydrolysis of cellulose, a major component of lignocellulosic biomass, to glucose monomers typically involves a very long reaction time (>24 h) and very harsh reaction conditions (>60 wt% sulfuric acid) due to its highly crystalline structure.[13] In order to tackle this problem, many researchers have applied the ball-milling pretreatment before the hydrolysis of cellulose.[14] Once the cellulose crystallinity is deconstructed by the mechanical pulverization, it is possible to use the cost-effective solid acid catalysts such as sulfonated carbons for achieving the high-yield production of glucose up to 80–90%.[15] Although ball-milling is an effective technique to reduce cellulose, its mechanical grinding characteristics raises several issues, including high energy consumption, prolonged milling time, and damage to cellulose samples and equipment due to excessive frictional heat and abrasion. The energy consumption can range from 9000 to 36 000 W kg^{-1} in the case of a planetary ball mill, and the milling time can exceed 4 days due to the structural rigidity of cellulose. These limitations hinder the commercial viability of ball-milling as a means of cellulose pretreatment.

As an alternative to the high energy-demanding ball-milling process, an ionic liquid (IL) pretreatment of cellulose has been studied by many researchers.[16] In the presence of ionic liquids, numerous hydrogen bonds in the cellulose can be broken or reduced due to their strong interaction with cations and anions of the ionic liquids, weakening the solid crystalline structure. Previous studies have mainly focused on the utilization of ionic liquid as a reaction medium to convert the dissolved cellulose in an ionic liquid directly into monosaccharides or other derivatives. This approach demonstrated the excellent conversion and yield.[17,18] However, the hydrolysis of cellulose in ionic liquids as

School of Chemical Engineering, Pusan National University, Busan 46241, Republic of Korea. E-mail: jh.jae@pusan.ac.kr; Tel: +82-51-510-2989

† Electronic supplementary information (ESI) available. See DOI: https://doi.org/10.1039/d2ra08224a

a solvent has the separation problem of sugar products and ionic liquids due to their high boiling points, which greatly increases the process cost. To solve this problem, a method of regeneration of cellulose by adding anti-solvents such as water to the dissolved cellulose in ILs was proposed by other researchers.[19–24] It has been shown that the addition of excess water results in the destruction of cellulose–ionic liquid bonds and subsequent reformation of cellulose–cellulose hydrogen bonding, thereby precipitating as a solid cellulose again. Due to the distorted conformation resulting from the destruction/reformation of the H-bondings between glucose monomers, the regenerated cellulose has amorphous form with a reduced degree of polymerization (DP).[25]

Multiple researchers have shown that regenerated celluloses from ionic liquids have enhanced hydrolysis kinetics than untreated cellulose. For instances, Zhao *et al.* reported that the cellulose regenerated from various chloride- and acetate-based ILs such as [BMIM]Cl exhibited 2 to 10 times faster rates for enzymatic hydrolysis than untreated cellulose.[24] Morales-delaRosa *et al.* compared the acid hydrolysis of cellulose regenerated from [EMIM]Cl with that of the untreated cellulose.[21] They found that the use of the homogeneous acid catalyst, phosphotungstic acid, resulted in the complete conversion of the regenerated cellulose within 5 h at 413 K with a high glucose yield of 87%, while the untreated cellulose exhibited only 24% cellulose conversion under the identical condition. Meanwhile, Lai *et al.* studied the solid acid-catalyzed hydrolysis of regenerated cellulose using sulfonated SBA-15 catalysts.[26] Compared to homogeneous acids, the relatively low glucose yield ~50% was obtained at 433 K. Kim *et al.* also reported the low glucose yield of ~35% when the cellulose treated in [BMIM]Cl is hydrolyzed over Nafion® NR50 catalyst presumably due to the limited accessibility of cellulose to the solid catalyst surface.[27]

Although previous studies have demonstrated the effectiveness of the dissolution/regeneration (DR) pretreatment for cellulose hydrolysis, there are still several unanswered questions as follows. First, there is no study on the direct comparison of the hydrolysis kinetics between the ball-milled and DR pretreated celluloses, making it difficult to estimate the level of efficiency of the DR process over the conventional ball-milling process. Second, the solid acid-catalyzed hydrolysis of DR pretreated cellulose was not optimized, having the relatively low yield of glucose (<50%). For instance, the most active solid acid catalyst for the cellulose hydrolysis was reported to be the sulfonated carbon catalyst, but this type of catalyst has not yet been applied to the DR-pretreated cellulose.[28] Third, although ILs can be recycled after the DR process, they are expensive, corrosive, and toxic, which limits their large-scale application. Thus, it would be interesting to expand the scope of the ILs for the DR process into an inexpensive and greener solvent system, *e.g.*, deep eutectic solvent (DES). DES is a eutectic mixture that has a lower melting point than its individual components. It is generally obtained by the complexation of a quaternary ammonium salt with a hydrogen bond donor (HBD) in which the latter can form intermolecular hydrogen bonds with the anions of the former, resulting in the decrease in the melting point. While ILs are formed from one type of discrete anion and cation, DESs can be formed from a eutectic mixture of a variety of an ionic and/or cationic species, rendering the wide tunability for their solvent properties.[29] Although the efficiency of the breaking of the hydrogen bonds of cellulose (*i.e.*, cellulose dissolution) is still lower with DESs than with ILs, choline chloride (ChCl) based DESs have shown the promising performance. Specifically, ChCl paired with the HBD of imidazole (Im) exhibited the best cellulose dissolution efficiency up to 4.5 wt%, while the toxicity of Im might be rather problematic.[30,31] ChCl paired with lactic acid is the greener DES system investigated widely for the delignification of a range of biomass feedstock.[31] Although its cellulose solubility is rather low (<2 wt%), it could be a desirable alternative to the toxic ILs. Thus, two DESs of the ChCl–Im and ChCl–LA were selected for the comparison with ILs in this study.

The objective of this paper is to investigate the hydrolysis of regenerated cellulose from ILs and DES using sulfonated carbon catalysts and compare their activity with the conventional ball-milled cellulose. For this purpose, two representative ILs for cellulose dissolution, 1-ethyl-3-methylimidazolium chloride ([EMIM]Cl) and 1,3-dimethylimidazolium dimethyl phosphate ([DMIM]DMP), and two choline chloride-based DESs were selected as the test samples. The sulfonated carbon catalysts were prepared by the thermal oxidation of the commercial activated carbon followed by sulfonation. The hydrolysis of cellulose was conducted at 150 °C for 12 h. In addition, the hydrolysis experiments in the presence of 100 bar-CO_2 was conducted to see if the carbon dioxide-induced carbonic acid can act as an acid co-catalyst to boost the hydrolysis of cellulose.

Experimental

Materials

α-Cellulose as a feedstock was purchased from Sigma-Aldrich (KOREA). The activated carbon, nitric acid (HNO_3, 70%) and sulfuric acid (H_2SO_4, 95–98%) were purchased from Sigma-Aldrich. 1-Ethyl-3-methylimidazolium chloride ([EMIM]Cl, 98%) and 1,3-dimethylimidazolium dimethyl phosphate ([DMIM]DMP, 98%) were purchased from Sigma-Aldrich. Lactic acid and choline chloride were also provided by Sigma-Aldrich.

Ball milling pretreatment of cellulose

Ball milling was performed to reduce crystallinity by mechanically breaking hydrogen bonds in cellulose. A ball milling equipment consisted of a general laboratory roller ball miller, a porcelain jar (3.6 L) and a zirconia ball (10 mm, 5 mm). For a typical experiment, 10 g of α-cellulose and 500 g of 10 mm, 5 mm zirconia ball were put in a porcelain jar, and the rotational speed (rpm) was fixed at 60 rpm. Cellulose and zirconia balls inside the porcelain jar fall by potential energy, collide with each other, and physically pulverize. The ball milling time lasted for 4 days to completely deconstruct the crystallinity of cellulose.

Preparation of deep eutectic solvents (DESs)

In the case of DES (ChCl : LA), lactic acid and choline chloride were put into a beaker at a molar ratio of 10 : 1. Then, stirring was performed at 70 °C until it becomes a transparent liquid. After that, the mixture was cooled to room temperature and stored at ambient condition. In the case of DES (ChCl : Im), imidazole and choline chloride were placed in a beaker in a molar ratio of 7 : 3. Then, the mixture was stirred at 90 °C until it becomes a liquid phase. The mixture was then cooled to room temperature and stored at ambient condition.

Cellulose dissolution/regeneration (DR) using ILs and DESs

The experiments were conducted as follows to obtain IL and DES-treated cellulose for comparison with ball-milled cellulose. The DR process of cellulose using ILs and DESs were performed as follows. First, 0.12 g of α-cellulose was added to 3 g of the prepared ILs or the DESs and stirred at 100 °C for 6 h to synthesize ionic cellulose. After cooling to room temperature, 100 mL of excess deionized water (DW) was added to the ionic cellulose and stirred at room temperature for 2 h for the precipitation of the regenerated cellulose. Then, centrifugation was performed for 5 min at 3000 rpm. After removing the supernatant in the centrifuged solution, it was dried in an oven at 100 °C for 12 h to obtain the powder phase regenerated cellulose. The chemical process of the DR treatment together with the chemical structure of ILs and DESs used in this study is depicted in Fig. 1. The overall reaction network is also provided in Fig. S1.†

Preparation of sulfonated carbon catalysts

A hydroxyl group (–OH), a carboxyl group (–COOH), a phenol structure (C_6H_5–OH), and a lactone group (–COO–) of the activated carbon (AC) were produced by the chemical treatment method as follows. First, 10 mL of 65% nitric acid was slowly add to 1 g of activated carbon drop by drop. Then, the solution was heat at 60 °C for 1 h while vigorously stirring. Subsequently, the carbon powder was separated by filtration followed by washing with excess distilled water until it becomes neutral. After that, the carbon sample was dried in a drying oven at 110 °C for 12 h and denoted as AC.

The AC sample was then used as a parent material for introducing a sulfonic group (–SO_3H). The synthesis method is as follows. First, 15 mL of 98% concentrated sulfuric acid was slowly added to 1 g of AC in water. Since –OH and –COOH groups can react with the oxygen and moisture in the atmosphere to cause a substitution reaction, all the synthesis experiments were conducted in a nitrogen atmosphere. The sample solution was stirred in a nitrogen atmosphere and heated to 200 °C for 24 h. After filtration, the carbon powder was washed with hot distilled water to remove the physically adsorbed SO_4^{2-}. Finally, it was dried in an oven at 110 °C for 12 h followed by calcination at 200 °C for 2 h in a nitrogen atmosphere. The final sample was then directly used for the hydrolysis experiments of cellulose.

Characterization of the regenerated cellulose and sulfonated carbon catalysts

XRD analysis was performed using Panalytical's X'pert³ Powder X-ray spectroscopy equipment to characterize the crystallinity of the pretreated cellulose and carbon catalysts. A diffraction pattern was obtained using an X-ray source of Cu K-α (λ = 1.54056 Å) operated at 40 kV and 30 mA. The scan rate was 5° per min, the scan step size was 0.02°, and the scan range was 5° to 60°. Handling of analysis and sample information was acquired using Highscore Plus software of X'pert³ analyzer. To check the particle size of the regenerated cellulose samples, SEM analysis was also carried out under the condition of an acceleration voltage of 15 kV using the ZEISS SUPRA 40 field emission scanning electron microscope. In the case of the cellulose sample, the reflection effect of the electron beam was enhanced by Pt coating. FT-IR analysis was performed with a Nicolet IS10 instrument (Thermo Scientific) to confirm the incorporation of the functional groups into the chemically treated carbon catalyst. The functional group spectrum of the carbon catalyst was analyzed in the wavelength range from 400 to 4000 cm^{-1}. To quantitatively analyze the amount of functional groups of the carbon catalyst, ICP-OES analysis was also

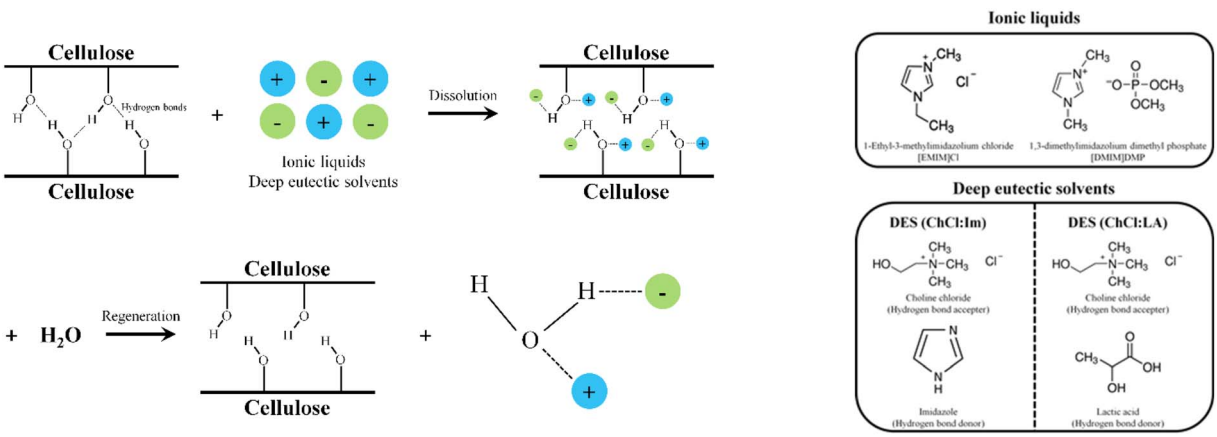

Fig. 1 Chemical process of the DR treatment (left) and chemical structures of ILs and DESs used in this study (right).

performed using the iCAP PRO instrument of Thermo Scientific.

Reaction methods

The hydrolysis of cellulose was performed in a 160 mL autoclave batch reactor equipped with four-blade paddle impellers (Inconel 625) and an electronic heater. For a typical experiment, 0.05 g of cellulose and 0.05 g of sulfonated carbon catalysts were placed in the reactor, and 40 mL of water was used as the solvent. The reactor was then pressurized with N_2 up to 30 bar. After setting the reactor pressure, its temperature was raised to 150 °C using four cartridge heaters mounted on the reactor wall and an electric furnace, and the stirring speed was fixed at 300 rpm. The reaction was maintained for 12 h from the time when the reactor reached the target temperature.

In case of the CO_2 addition experiment, the liquid CO_2 was introduced to the reactor using the HPLC pump at a constant feeding rate after charging the reactor with the reactant and water. The amount of CO_2 injected into the reactor was 100 bar at 35 °C. The final reactor pressure exceeded 200 bar when the reactor temperature was raised to 150 °C. Thus, the CO_2 in the reactor was in the supercritical state.

Product analysis was performed by High Performance Liquid Chromatography (HPLC). Agilent's HPLC 1200 Infinity instrument was used to analyze soluble sugar compounds and by-products, *i.e.*, sugar-decomposed products. For the column, Hi-Plex Ca (Duo), 300 × 6.5 mm was used, and the product yield was quantified based on an external calibration method. For the estimation of the cellulose conversion, the carbon content of the reactant solution before and after reactions were monitored by Total Organic Carbon (TOCs) analyzer. The cellulose conversion is defined as the total carbon amount of water-soluble products in the product solution divided by the amount of cellulosic carbon in the reactant. The glucose yield was estimated by the quantitative glucose data from HPLC analysis. The formula for calculating the cellulose conversion and glucose yield are as follows.

Cellulose conversion (%) = $100 \times B/A$

Glucose yield (%) = $100 \times C/A$

A: total amount of cellulosic carbon analyzed by TOCs.

B: total amount of water-soluble product carbon analyzed by TOCs.

C: total amount of carbon in the glucose product analyzed by HPLC.

Results and discussion

Characterization of the regenerated cellulose

The change in crystallinity of the regenerated cellulose samples after the dissolution in ILs and DES was analyzed by XRD and compared with the ball-milled cellulose. Fig. 2 shows the XRD results of the native and regenerated celluloses. When looking at the XRD graph of the native cellulose, the intense peaks appear at about $2\theta = 16°$ and 21°, which are the characteristic peaks for crystalline cellulose.[14] In contrast, an intensity of these peaks is largely decreased in the regenerated cellulose after IL pretreatment ([EMIM]Cl, [DMIM]DMP), indicating the effectiveness of IL treatment for the destruction of cellulose crystallinity as expected.[32] The DES treatment was also effective in reducing the cellulose crystallinity, showing the decrease of the main peaks for crystalline cellulose.[33] In particular, the treatment with DES (ChCl : Im) showed a more effective reduction in cellulose crystallinity than that of DES (ChCl : LA), suggesting that imidazole as a HBD is more effective in dissociating hydrogen bonds in cellulose than lactic acid as reported previously.[31,33] However, the degree of decrease in crystallinity of cellulose treated with DES (ChCl : Im) was still lower than those of the two ILs, showing the higher peak intensity at $2\theta = 16°$. The crystallinity reduction observed in ball-milled cellulose was also more substantial than those of celluloses treated with DES and comparable to those of celluloses treated with IL. This can be partially due to the effective reduction in the crystalline domain size by the mechanical pulverization of cellulose particles. Overall, the reduction efficiency in the cellulose crystallinity decreased in the following order, [EMIM]Cl = [DMIM]DMP > ball-milling > DES (ChCl : Im) > DES (ChCl : LA).

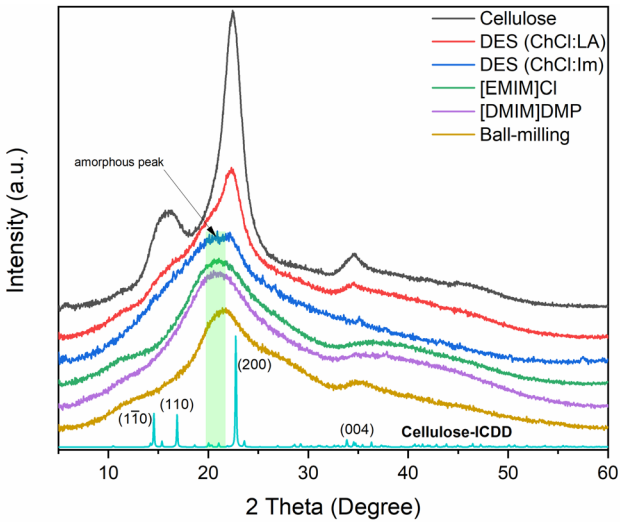

Fig. 2 XRD graph of pretreated cellulose: DES (ChCl : LA) (red), DES (ChCl : Im) (blue), [EMIM]Cl (green), [DMIM]DMP (pink) and ball-milling (yellow).

FE-SEM analysis was performed to characterize the particle size of cellulose after treatment with the ILs and DES. Fig. 3 shows the FE-SEM images of regenerated cellulose samples as well as the native and ball-milled celluloses. The native cellulose sample had an average particle size of 300 μm. In general, the average particle size of cellulose decreased largely after the treatment of ILs and DES. Specifically, cellulose treated with [EMIM]Cl and [DMIM]DMP had average particle sizes of 35–40 μm and 50–60 μm, respectively. On the other hand, DES-treated celluloses had relatively large particle sizes of 80–90 μm, compared to two IL treated samples. These particle size analysis results are consistent well with those of XRD measurements, in which the DES-treated sample has the higher crystallinity than IL-treated samples. It is though that large cellulose particles are initially fragmented to small cellulose molecules after the

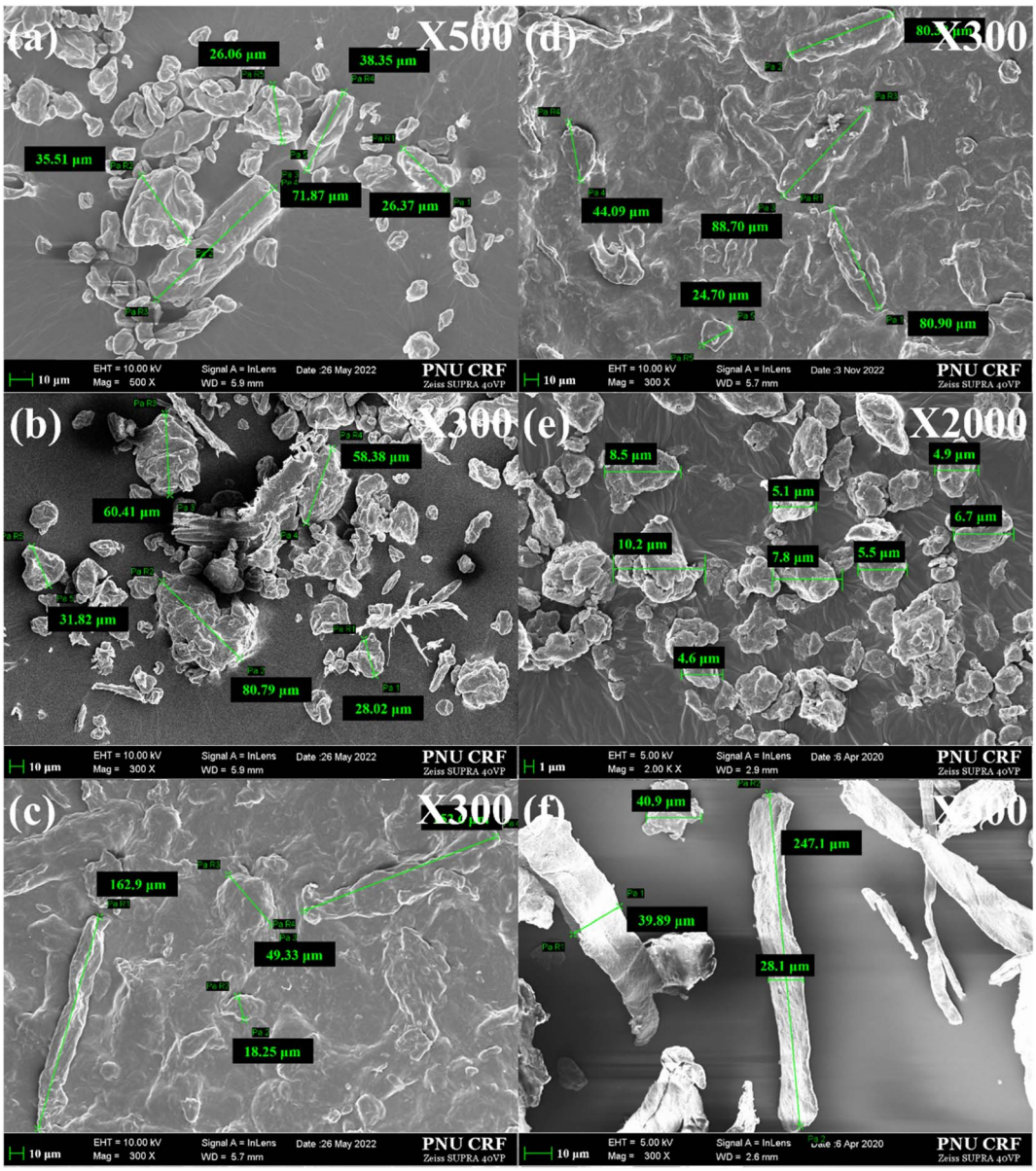

Fig. 3 FE-SEM image of cellulose treated with ILs and DES: [EMIM]Cl (a), [DMIM]DMP (b), DES (ChCl : LA) (c), DES (ChCl : Im) (d), ball-milling (e) and untreated cellulose (f).

dissolution with ILs and then reaggregate with the adjacent cellulose during the regeneration process of adding an excess of water, thereby forming the reduced particle size compared to untreated cellulose.[21] Meanwhile, the particle size of the ball-milled cellulose was much smaller than those of IL and DES-treated samples, showing ~10 μm average particle size. All of the pretreated cellulose samples underwent a significantly reduction in the size of particles compared to the original one (300 μm to 80–10 μm). Overall, the average particle size of the cellulose samples increases in the following order, ball-milling < [EMIM]Cl < [DMIM]DMP < DES (ChCl : Im) < DES (ChCl : LA). In addition, the morphology of cellulose underwent conspicuous changes depending on the pretreatment method. Untreated cellulose exhibited rough and irregular surfaces, retaining its long stick shape (average length of 300–500 μm). The ball-milled cellulose comprised ellipsoidal fine particles resulting from fine cleavage through mechanical grinding. The IL-treated cellulose samples consisted of various rod-shaped, plate-shaped, or irregular elliptical fine particles, while the DES-treated samples lost their particle characteristics due to fibrillation. It appeared that a huge lump-like cellulose was formed by the random regeneration of hydrogen bonds between adjacent cellulose molecules.

Characterization of the sulfonated carbon

Fig. 4 shows the FT-IR analysis results for the functional groups introduced into the prepared carbon catalyst. In general, –OH and –COOH groups are responsible for the chemical adsorption

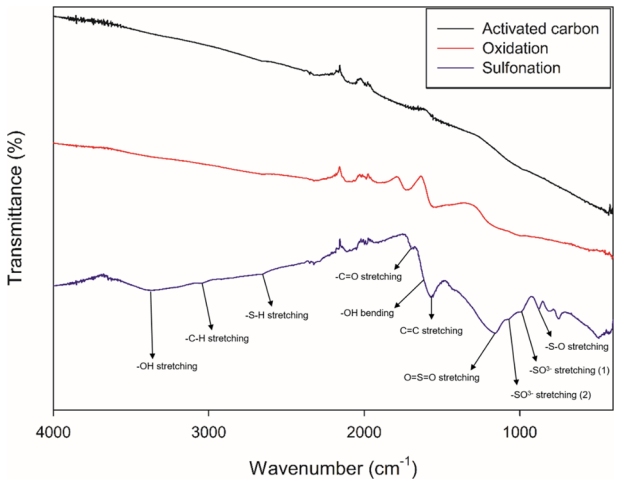

Fig. 4 FT-IR spectra of carbon catalysts with functional groups.

of cellulose, while $-SO_3H$ groups are the main active sites for the breaking of β-1,4-glycosidic bonds of cellulose.[34] For comparison, the FT-IR results of the native activated carbon (AC) and AC with only oxidation treatment are also provided. The native AC shows some very weak FT-IR peaks, indicating that it contains only few oxygen functional groups. However, in the case of the AC with oxidation, OH bonds at the wave number 950 and 1500 cm^{-1}, C–O bonds at 1230 cm^{-1}, C═O bonds at 1700 cm^{-1} and lactone bonds at 1750–1900 cm^{-1}, respectively, are clearly observed, confirming that the oxygen-functional groups are successfully produced after oxidation process.[34] In the case of sulfonation, it can be seen that oxidation peaks are amplified during sulfonation, while $-SO_3H$ bond-related peaks appear strongly at 500–1500 cm^{-1}.[35] Especially, the peak representing the $-SO_3H$ bond, at 1250 cm^{-1}, appears very strongly, confirming that the targeted $-SO_3H$ groups was well produced.[36]

Hydrolysis of regenerated cellulose

Hydrolysis of the regenerated cellulose was performed using the sulfonated carbon catalyst at 150 °C for 12 h. Fig. 5 shows the

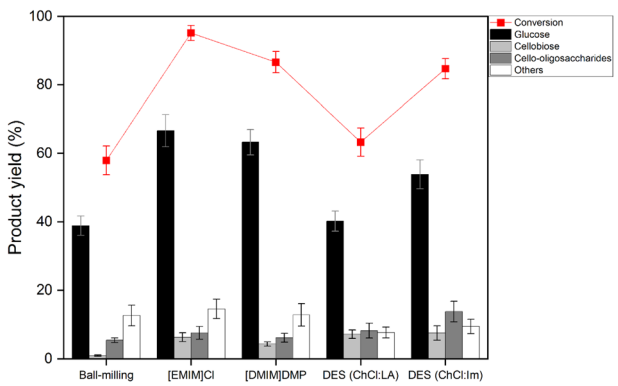

Fig. 5 Reaction results of pretreated cellulose (reaction condition: cellulose 0.05 g, catalyst 0.05 g, D. I. water 40 mL, temp. 150 °C, time 12 h).

conversion and product yields for the hydrolysis of the regenerated cellulose. Overall, when cellulose was treated with the ILs or the deep eutectic solvents, the conversion and the sugar yields were higher than those of the ball-milling treatment, indicating that the DR process increases the hydrolysis kinetics more effectively than the ball-milling treatment. This result is rather contradictory to the XRD and SEM results in which ball-milled cellulose has lower crystallinity and lower particle size than the DR-pretreated samples. It is thought that the hydrogen-bondings inside the core of the ball-milled cellulose particles would remain intact, even though the mechanical force breaks the outer surface hydrogen bonds of cellulose particles. In contrast, in the case of ILs and DES that chemically break hydrogen bonds, the hydrogen-bonding inside the core can be breakable through the access of small anions and cations.[22] Although the hydrogen bonds are reformed during the regeneration process, the structural hardness would be weakened by the distorted conformation of glucose monomers, making it more effective toward the hydrolytic decomposition.[19]

Specifically, the conventional ball-milled cellulose exhibited a low conversion of ~58% and a low glucose yield of ~40%. When [EMIM]Cl was used, the highest cellulose conversion of ~97% and the highest glucose yield of ~68% were achieved. In contrast, [DMIM]DMP showed a ~85% conversion a ~62% monosaccharide yield, which are slightly lower than those of [EMIM]Cl. Since the phosphate-based anion exhibits lower electronegativity than the chloride anion, the decomposition rate of hydrogen bonds in cellulose would be lower, which, in turn, results in the lower hydrolysis efficiency with phosphate.[27] In the case of the cellulose sample treated with DES (ChCl : LA), it has conversion (~60%) and monosaccharide yield (~40%) much lower than those of IL treatment. However, when the cellulose sample was treated with the DES (ChCl : Im), it showed improved conversion (~85%) and enhanced monosaccharide yield (~53%). The observed hydrolysis activity trend is well correlated with the degree of the crystallinity reduction of cellulose and, in turn, the solvent power of the DES. In general, the solvation performance depends on the various properties of DES, including the hydrogen bond basicity, hydrogen bond acidity, dipolarity/polarizability, *etc.*[37] According to Ren *et al.*, the cellulose dissolution efficiency is mainly controlled by the hydrogen bond basicity of the DES rather than other parameters because the essence of the cellulose dissolution is the disruption of the hydrogen bonds in cellulose.[30] Thus, the higher hydrogen bond basicity of the DES–Im induced by π–π conjugative effect of the imidazole ring may be the reason for the higher solubility of cellulose, resulting in the higher hydrolysis activity toward glucose production.

The overall hydrolysis efficiency of the DES-treated cellulose is lower than that of IL. This is due to the lower cellulose dissolution efficiency of DES as confirmed by XRD and SEM measurements. The hydrolysis activity of the DES (ChCl : Im) is, however, comparable to that of the second place IL, *i.e.*, [DMIM]DMP, although its toxic characteristic nullifies the environmental benefit over ILs. The eco-friendly natural DES (ChCl : LA) exhibited much lower activity for cellulose hydrolysis, suggesting that the new DES system for cellulose dissolution is needed.

In addition, it is worth paying attention that the DES-treated sample had the advantages over the IL-treated samples in terms of product selectivity; it has higher yields of valuable cellobiose and oligosaccharides and lower production of sugar decomposed products, including 5-hydroxymethylfurfural (5-HMF), formic acid and levulinic acid.[38] The detailed distribution of these decomposed products are displayed in Fig. S2.† In particular, when compared to the ball-milled cellulose, the DES-treated samples still exhibited lower selectivity to sugar decomposed products even at similar conversion (~60%), suggesting their structural resistance to the secondary decomposition reactions.

In order to analyze the detailed composition of the oligosaccharides, MALDI-TOF analysis was also performed. Fig. 6 shows MALDI-TOF analysis spectra of hydrolysis products obtained from IL- and DES-treated cellulose samples. All samples mainly included tri-, tetra- and pentasaccharide as oligosaccharide products. The relative abundance of individual oligosaccharides differed depending on the cellulose samples. Especially, the selectivity of tetra- and pentasaccharide for the DES (ChCl : LA)-treated samples were relatively higher than those for IL-treated samples. Recently, those short-chain cello-oligosaccharides are receiving increasing attention due to their wide application in pharmaceutics, agriculture, food and chemicals. In this respect, the selectivity enhancement toward the oligosaccharides in cellulose hydrolysis is of growing importance.[39,40] Especially, compared to the ball-milling treatment, IL- or DES treatment allows for more production of valuable oligosaccharides which can be considered as an important benefit of the DR treatment.

Fig. 7 shows hydrolysis reaction results in the presence of supercritical CO_2, while Fig. 8 shows MALDI-TOF spectra of the hydrolysis products. The reaction condition was identical to the previous experiment except that supercritical carbon dioxide was injected at room temperature to 100 bar. We have previously shown that supercritical carbon dioxide-induced carbonic acid is sufficiently acidic to catalyze the hydrolytic depolymerization of lignin to biocrude oils.[41] According to the calculation based on the thermodynamic model reported by Duan *et al.*,[42] the pH of carbonic acid at 150 °C and 100 bar-CO_2 is nearly 3.0. Thus, we envisioned that the added CO_2 can act as an acid co-catalyst for the enhanced hydrolysis of the regenerated cellulose, particularly for the water-insoluble fraction of cellulose due to the homogeneous nature of the carbonic acid. Although several researchers have reported on the use of high-pressure CO_2 as an acid catalyst for biomass conversion such as the dehydrative cyclization of biomass-derived polyols,[43,44] there is no report on the use of supercritical CO_2 for the hydrolysis of cellulose.

The initial experiments on the conversion of cellulose with and without 100 bar-CO_2 confirmed the catalytic effect of CO_2, showing the increased glucose yield (see Fig. S3†). Notably, in the presence of the sulfonated carbon catalyst, the addition of supercritical CO_2 enhanced the cellulose conversion and glucose yields significantly. In case of the [EMIM]Cl treated cellulose, the cellulose conversion reached ~100%, and the glucose yield increased to ~82%, suggesting the promoting role

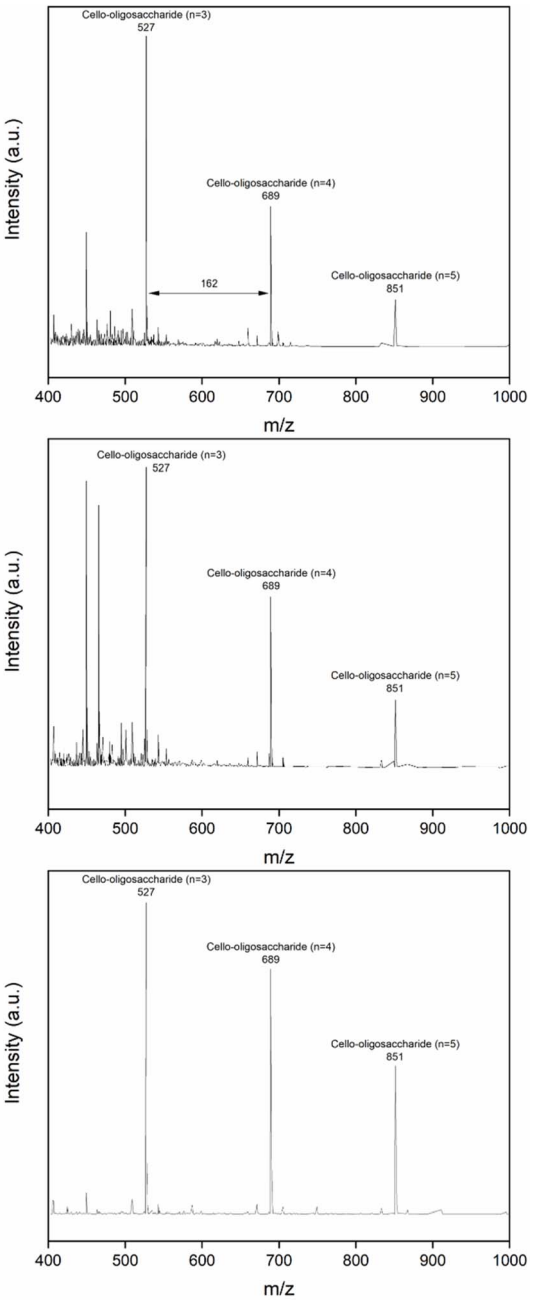

Fig. 6 MALDI-TOF analysis of pretreated cellulosic hydrolysis products: [EMIM]Cl (top), [DMIM]DMP (middle), DES (ChCl : LA) (bottom).

of carbon dioxide-induced carbonic acid in the cellulose hydrolysis. Similarly, [MMIM]DMP-treated sample exhibited the enhanced hydrolysis kinetics, having ~78% glucose yield at nearly ~100% conversion. The obtained glucose yield of the [MMIM]DMP-treated cellulose was, however, still lower than that of the [EMIM]Cl treated cellulose as in the case of the reaction without CO_2. An increase in the hydrolysis activity was also significant in the case of the DES-treated sample. The conversion of the DES (ChCl : LA)-treated cellulose increased from 60% to 100%, and the glucose yield increased from 40% to 62% with an addition of CO_2. Similarly, the conversion of the

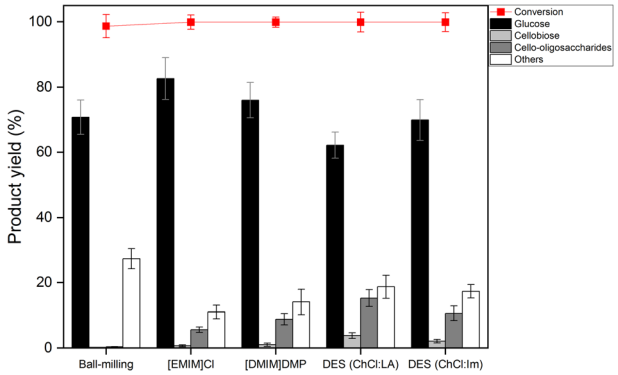

Fig. 7 Reaction results of pretreated cellulose with supercritical CO_2 (reaction condition: cellulose 0.05 g, catalyst 0.05 g, D. I. water 40 mL, temp. 150 °C, time 12 h, supercritical CO_2 injection 100 bar).

cellulose treated with DES (ChCl : Im) increased from 83% to 100%, and the glucose yield also increased from 53% to 70%. Compared to two IL-treated samples, the DES-treated samples showed the lower glucose yields, but higher cellobiose (~5%) and oligosaccharide yields (~20%), indicating its slower hydrolysis rate. The MALDI-TOF analysis results were also consistent with the yield data. The peak intensity of oligosaccharides in the DES (ChCl : LA)-treated sample was much higher than those in IL-treated samples, as shown in Fig. 7. In addition, high-carbon-number hexasaccharide was also newly detected as the major product. This result suggests that the DES-treatment can be the good option if the target products from the hydrolysis of cellulose are cellobiose or oligosaccharides.

The ball-milled cellulose also showed the enhanced hydrolysis kinetics with an addition of CO_2, giving ~100% conversion and ~70% glucose yield. Notably, the glucose yield of the ball-milled cellulose is higher than those of the DES-treated ones. In the case of the ball-milled cellulose, there was no formation of cellobiose and oligosaccharides, and the sugar-decomposed products such as levulinic acid were produced with a very high yield (~25%), while the DES-treated samples have very high yields of oligosaccharides and low yields of levulinic acid. This distinct product selectivity of the ball-milled cellulose likely arises from its structural differences from the DES-treated cellulose, thereby impacting the hydrolysis chemistry. Specifically, Chen *et al.* reported that the activation energy required to cleave the glycosidic bonds increases with the decrease in the molecular size of the cello-oligosaccharides.[45] Thus, in the case of the DES-treated sample, the formation of glucose appears to proceed *via* the formation of cello-oligosaccharide intermediates by the preferential cleavage of the middle chains of the cellulose, resulting in the slower hydrolysis kinetics toward glucose production. In contrast, in the ball-milled sample, glucose may be produced directly from cellulose due to the preferential attack of the end chains of the cellulose. The ball-milled cellulose has more condensed structure so that the interaction of the carbon catalyst surface can be limited to the end chains of the cellulose. Once glucose is formed, it can easily undergo the secondary dehydration reaction to 5-HMF and LA.

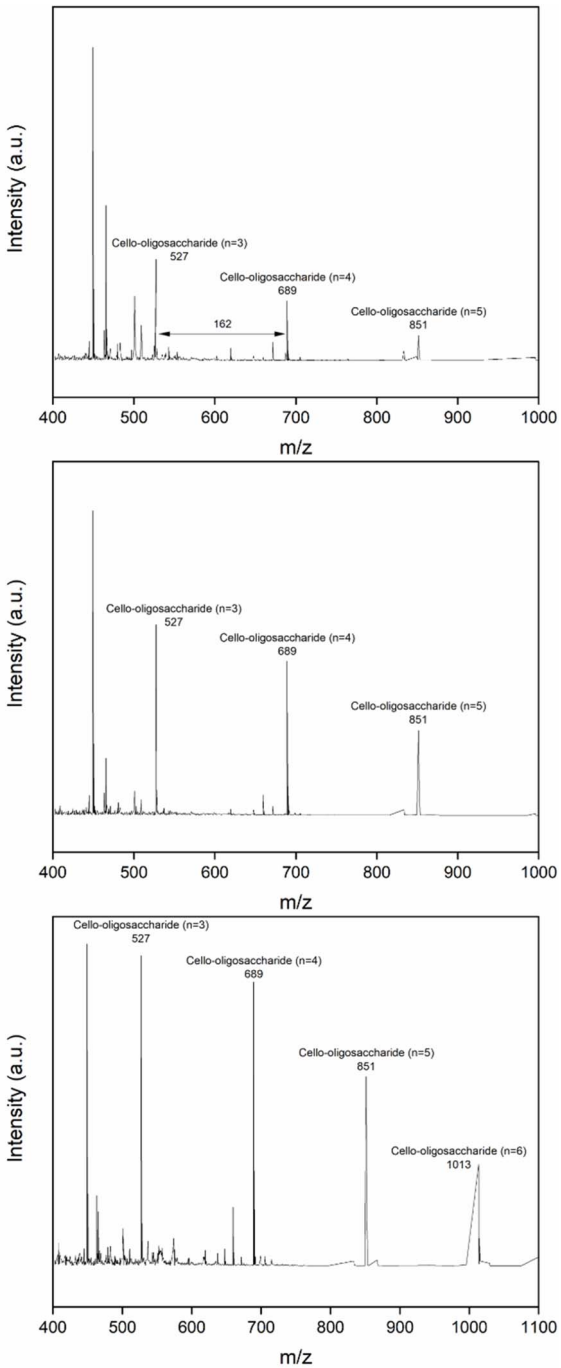

Fig. 8 MALDI-TOF analysis of hydrolysis products using pretreated cellulose and supercritical CO_2: [EMIM]Cl (top), [DMIM]DMP (middle), DES (ChCl : LA) (bottom).

Finally, Fig. 9 shows the by-product distribution obtained from the cellulose hydrolysis in the presence of supercritical CO_2. Compared to the reaction without CO_2, the formation of 5-HMF was significantly reduced, while the formation of levulinic acid and formic acid were increased substantially for all cellulose samples. This suggest that supercritical CO_2-derived carbonic acids accelerated the rehydration of 5-HMF to levulinic acid and formic acid, confirming its Brønsted acidity.

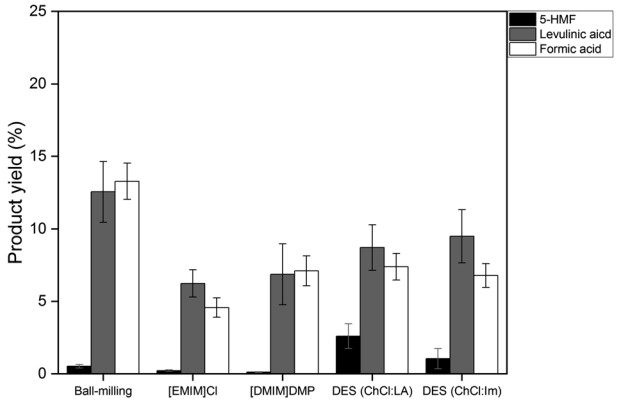

Fig. 9 The by-product distribution obtained from the cellulose hydrolysis with supercritical CO_2 (reaction condition: cellulose 0.05 g, catalyst 0.05 g, D. I. water 40 mL, temp. 150 °C, time 12 h, supercritical CO_2 injection 100 bar).

Overall, this study demonstrated that the cellulose DR pretreatment using the ILs and the DESs have superior kinetics for cellulose hydrolysis to the conventional ball milling treatment, suggesting a possibility to replace the current high energy-demanding ball-milling process with the energy-saving IL treatment. Moreover, compared to the results reported by other researchers using either ball-milling or IL pretreatments, the glucose yield obtained with the DR pretreatment is higher (see Table S1†). Between DES and IL-treated samples, the IL treatment shows the faster hydrolysis kinetics toward the monosaccharide production than the DES treatment due to their effective destruction of cellulose crystallinity induced by high solvation ability. The toxic DES (ChCl : Im) have comparable hydrolysis activity to the ILs, while the green and natural DES (ChCl : LA) exhibits relatively low hydrolysis activity due to their poor solvation efficiency, suggesting that the development of new DES system with high efficiency for cellulose dissolution is needed to realize the eco-friendly and energy-saving hydrolysis process for cellulose. Importantly, the DES treatment also demonstrated the advantage over the ball-milling treatment in terms of product selectivity, having the higher selectivity toward valuable short-chain cello-oligosaccharides.

Conclusions

In conclusion, the hydrolysis kinetics of the regenerated cellulose from ILs and DES were examined using sulfonated carbon catalysts and compared with the conventional ball-milled cellulose. The XRD and SEM analyses of the regenerated cellulose revealed that both IL and DES treatments are effective in destructing the cellulose crystallinity and reducing the particle size significantly. However, the level of crystallinity reduction of the DES-treated samples was somewhat lower than that of the ball-milled cellulose. The overall pretreatment efficiency decreased in the order of [EMIM]Cl = [DMIM]DMP > ball-milling > DES (ChCl : Im) > DES (ChCl : LA). The hydrolysis reaction results at 150 °C showed that the IL-treated two cellulose samples exhibited considerably higher conversion and higher glucose yield than the conventional ball-milled cellulose (60–70% *vs.* 40% glucose yield). Between ILs, [EMIM]Cl, a chloride-based ionic liquid, showed the higher hydrolysis efficiency than [DMIM]DMP, a phosphate-based ionic liquid, due to the strong electronegativity of chloride anion, which is, in turn, more effective for the destruction of hydrogen bonding in cellulose. In the case of DES-treatment, the DES (ChCl : Im)-treated cellulose exhibited the higher hydrolysis efficiency than the DES (ChCl : LA)-treated one (53% *vs.* 40% glucose yield) due to its high solvation ability induced by the high hydrogen basicity of Im. The overall hydrolysis activity of the DESs was still higher than that of the ball-milled one, suggesting the more effective deformation of cellulose crystallinity in the DES-treated sample unlike the XRD data. In general, the hydrolysis activity trend of the regenerated cellulose was correlated with the degree of crystallinity reduction of cellulose. When hydrolysis reactions were conducted in the presence of 100 bar-CO_2 with the sulfonated carbon catalyst, the hydrolysis activity of all cellulose samples (~nearly 100% conversion) significantly enhanced compared to those without an addition of CO_2, suggesting the synergic role of supercritical CO_2-induced carbonic acid as an acid co-catalyst in enhancing the hydrolysis kinetics. Compared to the ball-milled cellulose, the IL- and DES-treated cellulose were more selective toward the formation of the desired sugar products (either mono- or oligosaccharides) with far less formation of the undesired sugar decomposition products, suggesting the structural difference between the ball-milled and the regenerated celluloses. The highest glucose yield of ~82% was successfully obtained with the [EMIM]Cl-treated cellulose.

Author contributions

H. W. K. and S. S. conducted experiments and analyzed the experimental data. J. W. K. validated the data and revised the manuscript. H. W. K. and J. J. designed the experiments and wrote the main manuscript text. All authors reviewed the manuscript.

Conflicts of interest

The authors have no relevant financial or non-financial interests to disclose.

Acknowledgements

This research was supported by the Technology Development Program to Solve Climate Changes of the National Research Foundation (NRF) funded by the Korea Government (MSIT) (2020M1A2A2079801) and by the Korea Institute of Energy Technology Evaluation and Planning (KETEP) grant funded by the Korea government (MOTIE) (20214000000140, Graduate School of Convergence for Clean Energy Integrated Power Generation). We also gratefully acknowledge the financial support from the National Research Foundation (NRF) funded by the Korea Government (MSIT) (2022R1A2C1013376).

Notes and references

1 V. Ashokkumar, R. Venkatkarthick, S. Jayashree, S. Chuetor, S. Dharmaraj, G. Kumar, W.-H. Chen and C. Ngamcharussrivichai, *Bioresour. Technol.*, 2022, **344**, 126195.
2 A. S. Jatoi, S. A. Abbasi, Z. Hashmi, A. K. Shah, M. S. Alam, Z. A. Bhatti, G. Maitlo, S. Hussain, G. A. Khandro and M. A. Usto, *Biomass Convers. Biorefin.*, 2021, 1–13.
3 P. K. Maurya, S. Mondal, V. Kumar and S. P. Singh, *Environ. Sci. Pollut. Res.*, 2021, **28**, 49327–49342.
4 R. K. Srivastava, N. P. Shetti, K. R. Reddy, E. E. Kwon, M. N. Nadagouda and T. M. Aminabhavi, *Environ. Pollut.*, 2021, **276**, 116731.
5 R. Gerardy, D. P. Debecker, J. Estager, P. Luis and J.-C. M. Monbaliu, *Chem. Rev.*, 2020, **120**, 7219–7347.
6 W. Jin, L. Pastor-Pérez, J. Yu, J. A. Odriozola, S. Gu and T. Reina, *Curr. Opin. Green Sustainable Chem.*, 2020, **23**, 1–9.
7 M. Sharifzadeh, M. Sadeqzadeh, M. Guo, T. N. Borhani, N. M. Konda, M. C. Garcia, L. Wang, J. Hallett and N. Shah, *Prog. Energy Combust. Sci.*, 2019, **71**, 1–80.
8 J. C. Solarte-Toro, J. A. González-Aguirre, J. A. P. Giraldo and C. A. C. Alzate, *Renewable Sustainable Energy Rev.*, 2021, **136**, 110376.
9 S. Wang, H. Li and M. Wu, *J. Cleaner Prod.*, 2021, **303**, 126825.
10 A. Athaley, P. Annam, B. Saha and M. Ierapetritou, *Comput. Chem. Eng.*, 2019, **121**, 685–695.
11 J. Q. Bond, A. A. Upadhye, H. Olcay, G. A. Tompsett, J. Jae, R. Xing, D. M. Alonso, D. Wang, T. Zhang and R. Kumar, *Energy Environ. Sci.*, 2014, **7**, 1500–1523.
12 S. Chovau, D. Degrauwe and B. Van der Bruggen, *Renewable Sustainable Energy Rev.*, 2013, **26**, 307–321.
13 Y. P. Wijaya, R. D. D. Putra, V. T. Widyaya, J.-M. Ha, D. J. Suh and C. S. Kim, *Bioresour. Technol.*, 2014, **164**, 221–231.
14 H. Zhao, J. H. Kwak, Y. Wang, J. A. Franz, J. M. White and J. E. Holladay, *Energy Fuels*, 2006, **20**, 807–811.
15 J. Pang, A. Wang, M. Zheng and T. Zhang, *Chem. Commun.*, 2010, **46**, 6935–6937.
16 H. Wang, G. Gurau and R. D. Rogers, *Chem. Soc. Rev.*, 2012, **41**, 1519–1537.
17 S. J. Dee and A. T. Bell, *ChemSusChem*, 2011, **4**, 1166–1173.
18 Y.-Y. Bai, L.-P. Xiao and R.-C. Sun, *Cellulose*, 2014, **21**, 2327–2336.
19 K. M. Gupta, Z. Hu and J. Jiang, *RSC Adv.*, 2013, **3**, 12794–12801.
20 S. Morales-delaRosa, J. M. Campos-Martin and J. L. Fierro, *Catal. Today*, 2018, **302**, 87–93.
21 S. Morales-delaRosa, J. M. Campos-Martin and J. L. Fierro, *ChemSusChem*, 2014, **7**, 3467–3475.
22 R. P. Swatloski, S. K. Spear, J. D. Holbrey and R. D. Rogers, *J. Am. Chem. Soc.*, 2002, **124**, 4974–4975.
23 F. Zhang and Z. Fang, *Bioresour. Technol.*, 2012, **124**, 440–445.
24 H. Zhao, C. L. Jones, G. A. Baker, S. Xia, O. Olubajo and V. N. Person, *J. Biotechnol.*, 2009, **139**, 47–54.
25 L. Hu, L. Lin, Z. Wu, S. Zhou and S. Liu, *Appl. Catal., B*, 2015, **174–175**, 225–243.
26 D.-M. Lai, L. Deng, Q.-X. Guo and Y. Fu, *Energy Environ. Sci.*, 2011, **4**, 3552–3557.
27 S.-J. Kim, A. A. Dwiatmoko, J. W. Choi, Y.-W. Suh, D. J. Suh and M. Oh, *Bioresour. Technol.*, 2010, **101**, 8273–8279.
28 A. Onda, T. Ochi and K. Yanagisawa, *Green Chem.*, 2008, **10**, 1033–1037.
29 E. L. Smith, A. P. Abbott and K. S. Ryder, *Chem. Rev.*, 2014, **114**, 11060–11082.
30 H. Ren, C. Chen, Q. Wang, D. Zhao and S. Guo, *BioResources*, 2016, **11**, 5435–5451.
31 M. Zdanowicz, K. Wilpiszewska and T. Spychaj, *Carbohydr. Polym.*, 2018, **200**, 361–380.
32 A. Pinkert, K. N. Marsh, S. Pang and M. P. Staiger, *Chem. Rev.*, 2009, **109**, 6712–6728.
33 Y.-L. Chen, X. Zhang, T.-T. You and F. Xu, *Cellulose*, 2019, **26**, 205–213.
34 S. Suganuma, K. Nakajima, M. Kitano, D. Yamaguchi, H. Kato, S. Hayashi and M. Hara, *J. Am. Chem. Soc.*, 2008, **130**, 12787–12793.
35 T. T. Vi Tran, S. Kongparakul, P. Reubroycharoen, G. Guan, M. H. Nguyen, N. Chanlek and C. Samart, *Environ. Prog. Sustainable Energy*, 2018, **37**, 1455–1461.
36 M. Liu, S. Jia, Y. Gong, C. Song and X. Guo, *Ind. Eng. Chem. Res.*, 2013, **52**, 8167–8173.
37 H. Xu, Y. Kong, J. Peng, X. Song, Y. Liu, Z. Su, B. Li, C. Gao and W. Tian, *Bioresour. Technol.*, 2021, **319**, 124209.
38 R. Weingarten, W. C. Conner and G. W. Huber, *Energy Environ. Sci.*, 2012, **5**, 7559–7574.
39 P. Chen, A. Shrotri and A. Fukuoka, *Appl. Catal., A*, 2021, **621**, 118177.
40 C. Zhong, C. Ukowitz, K. J. Domig and B. Nidetzky, *J. Agric. Food Chem.*, 2020, **68**, 8557–8567.
41 H. U. Kim, J. W. Kim, N. T. Tran, S. O. Limarta, J.-M. Ha, Y.-K. Park and J. Jae, *Energy Convers. Manage.*, 2022, **261**, 115607.
42 Z. Duan and R. Sun, *Chem. Geol.*, 2003, **193**, 257–271.
43 S. Jing, X. Cao, L. Zhong, X. Peng, X. Zhang, S. Wang and R. Sun, *ACS Sustainable Chem. Eng.*, 2016, **4**, 4146–4155.
44 A. Yamaguchi, N. Hiyoshi, O. Sato, K. K. Bando and M. Shirai, *Green Chem.*, 2009, **11**, 48–52.
45 P. Chen, A. Shrotri and A. Fukuoka, *Catal. Sci. Technol.*, 2020, **10**, 4593–4601.